Introduction of a surface characterization parameter Sdr_{prime} for analysis of re-entrant features

[1]A. Townsend, [1]L. Pagani, [1]P. J. Scott, [1]L. Blunt

[1]EPSRC Future Metrology Hub, School of Computing and Engineering, University of Huddersfield, West Yorkshire, UK

A.townsend@hud.ac.uk +44 (0) 1484 472252

Abstract

Producing components using metal additive manufacturing processes, such as powder bed fusion, presents manufacturing and measurement challenges, but also significant opportunities. The as-built surface may include overhanging (re-entrant) features not intentionally included in the design, but that aid in component functionality. In addition, the additive manufacturing process presents opportunities to design and manufacture re-entrant features intentionally. Re-entrant features increase the specific surface area and, in addition, produce mechanical locking to the surface. These re-entrant features may be intended to improve surface performance in areas such as biological cell attachment, coating adhesion, electrical capacitance and battery plate design, fluid flow and material cooling. Re-entrant features may prove difficult or impossible to measure and characterise using conventional line-of-sight surface metrology instrumentation, however the correct measurement of these surfaces may be vital for functional optimisation. X-ray computed tomography *does* have the ability to image internal and re-entrant features. This paper reports on the measurement of re-entrant features using X-ray computed tomography and the extraction of actual surface area information (including re-entrant surfaces) from sample additively manufactured surfaces. A proposed new surface texture parameter, Sdr_{prime}, is discussed. This parameter is applicable to true 3D data, including re-entrant features, and is intended to relate directly to the component surface functional performance. The errors produced when using line-of-sight instruments and height map parameter generation per ISO 25178-2 to evaluate surfaces that include re-entrant features are discussed. Measurement results for electron beam melting and selective laser melting additively manufactured components, together with simulated structured surfaces, are presented.

Keywords

X-ray computed tomography

Additive manufacturing

ISO 25178

Surface texture

Re-entrant surfaces

1

1   Introduction

Electron Beam Melting (EBM) and Selective Laser Melting (SLM) metal powder bed fusion additive manufacturing (AM) techniques often generate surfaces containing re-entrant features such as overhangs and undercuts (see Fig.1(a)). Re-entrant planar surface features are characterised by two or greater z height values for an (x,y) position (see Fig.1(c)).
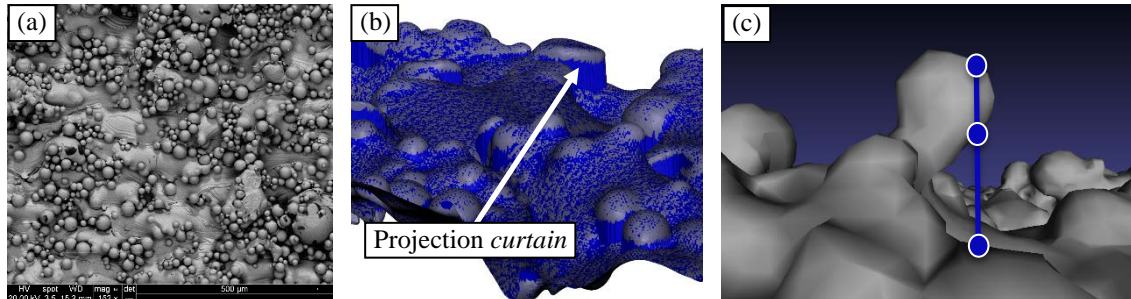
Fig.1 (a) Typical SLM side surface, (b) surface showing projection *curtains*, (c) re-entrant surface showing three z positions at one (x,y) location

These as-built features, a by-product of the AM layer-by-layer deposition process, may have functional advantages. Importantly, one significant advantage AM systems have, when compared to conventional subtractive processes such as milling and turning, is the ability to manufacture components with intentional, designed-in, re-entrant features at scales matched to the functional requirements. Manufacturing components with these features will provide advantages based on two properties produced by such features: firstly, re-entrant features increase the specific surface area: that is, an increase in the total surface areas for a given planar envelope area or component volume and secondly the ability to mechanically lock to the re-entrant surface. Increased surface area for a given planer area may have applications in battery and capacitor plate design where the surface contact area between liquid or gel electrolyte and the plate may be increased [1]. There may be applications in cooling and fluid flow where an increase in contact surface area provides greater volumetric efficiency [2] and medical applications such as orthopedic and dental implants where osseo integration between implant and tissue may be enhanced by the increased surface area [3]. These medical applications, and other applications such as paint and coating adhesion, may also be enhanced by the second property of re-entrant features that can be designed-in: the ability to mechanically lock to the surface. Dovetail joints used in woodworking are an example of mechanical locking due to designed shape.

Conventional surface topography measurement techniques, such as optical focus variation or confocal microscopy, mechanical stylus or CMM probing have a limited ability to measure internal or re-entrant features and can be considered "line-of-sight techniques". The surface data produced by such techniques is generally created as a height map, with a single z value corresponding to a specific (x, y) position. Surfaces between steps are interpolated, producing surface *curtains* at re-entrant features, see Fig.1(b). Characterisation of a re-entrant surface using line-of-sight measurement instrumentation and using height map analysis may, depending upon the surface texture parameter evaluated, produce significant errors. X-ray computed tomography (CT), used in this study, has no such line-of-sight restrictions and has been used successfully for the measurement of internal surfaces [4, 5], dimensions [6, 7] and porosity [8]. CT data is true 3D data, consisting of (x, y, z) co-ordinate information.

A new surface characterisation measurement parameter, Sdr_{prime}, is proposed here with the ability to extract surface information from true 3D data, such as that obtained using CT, which includes data for re-entrant surfaces. Sdr_{prime} is the percentage of additional surface (including re-entrant surfaces) contributed by the texture as compared to the area of a plane the size of the envelope area, therefore Sdr_{prime} relates directly to the specific surface area. Sdr_{prime} is computed as

$$Sdr_{prime} = \frac{1}{A_{prime}} \left(\iint_{D_S} \| \boldsymbol{r}_u(u,v) \times \boldsymbol{r}_v(u,v) \| \, du \, dv - A_{prime} \right)$$

where $\boldsymbol{r}(u,v)$ is the measured surface, described by a parametric function

$$\boldsymbol{r}(u,v) = \begin{cases} x = x(u,v) \\ y = y(u,v), \\ z = z(u,v) \end{cases}$$

$\boldsymbol{r}_\bullet(u,v)$ is the partial derivative in $\bullet$ direction, D_S is the domain of the measured surface and A_{prime} is the envelope area. Sdr_{prime} relates directly to the ISO 25178-2 [9] hybrid parameter Sdr, (called Sdr_{ISO} here for clarity) the developed interfacial area ratio, expressed as the percentage of additional area contributed by the texture as compared to a plane the size of the envelope area, which has application for height map (grid) data and does *not* have application to true 3D data, and so, significantly, *cannot* account for data from re-entrant features. Sdr_{ISO} is computed as

$$Sdr_{ISO} = \frac{1}{A} \left[\iint_A \left(\sqrt{1 + z_x^2 + z_y^2} - 1 \right) dx \, dy \right]$$

Pagani et al. [10] proposed a generalisation of the Sdr parameter (called Sdr_{mesh} here for clarity) that computes the percentage of additional surface contributed by the texture as compared to the *form* area (not the envelope area), computed as

$$Sdr_{mesh} = \frac{1}{A} \left(\iint_{D_S} \| \boldsymbol{r}_u(u,v) \times \boldsymbol{r}_v(u,v) \| \, du \, dv - A \right)$$

where A is the form area. Fig.2 shows a two-dimensional (profile) representation of the form area and envelope area for a generated surface section. The envelope area, used in the calculation of Sdr_{ISO} and Sdr_{prime}, represented by profile length (a) in Fig.2, is not surface-structure dependent and relates directly to the component dimensions. The form area, used for the calculation of Sdr_{mesh}, represented by profile length $(a + b + c)$ in Fig.2, is the total area of all surfaces (upward and downward facing) projected onto the measurement plane. The form area is therefore structure dependent and the presence of re-entrant features will increase the form area, but will not change envelope area.
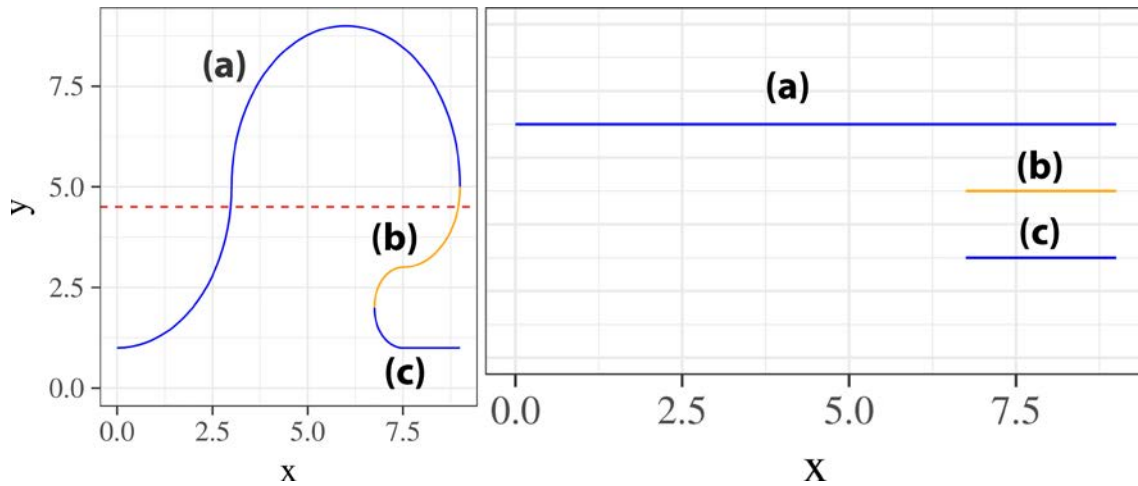
Fig.2 Profile representations of envelope and form areas (a) surface section profile, (b) envelope length (a) and form length (a+b+c)

It should be noted that if there are no re-entrant features the form area is equivalent to the envelope area and the values of Sdr_{ISO}, Sdr_{prime} and Sdr_{mesh} are equivalent.

1.1 Why use Sdr_{prime}?

The significant advantages of parameter Sdr_{prime} over Sdr_{ISO} and Sdr_{mesh} are, firstly, that the parameter relates directly to the physical envelope of the measured component (Sdr_{ISO} does also, but Sdr_{mesh} does not) and, secondly, that Sdr_{prime} has the ability to include all surface features, including re-entrant features (Sdr_{mesh} does also, but Sdr_{ISO} does not). Of the three Sdr parameters, Sdr_{prime} is the only one that reports the actual percentage increase of the designed surface area due to the surface texture in relation to the physical envelope of the measured component, making it most functionally useful. As Sdr_{prime} is the percentage of surface area above the area of a plane the size of the envelope area, calculation of the *actual* surface area of a component surface is simply a matter of multiplying the envelope area value by $(Sdr_{prime}/100) + 1$. Values of Sdr_{mesh} will be reported here for completeness, but the primary comparison here is between the ISO 25178-2 parameter Sdr (called Sdr_{ISO} in this paper for clarity) and Sdr_{prime}, as Sdr_{prime} has a more direct relation to functional performance.

2 Methodology

This work reports on the measurement and analysis of the as-built surfaces of two AM components: a 3 x 2 mm area extracted from the planar side-surface of a 20 x 12 x 10) mm medical implant and a section of a (3 x 2 x 2) mm bio-active lattice structure with nominally cylindrical, approximately 0.5 mm diameter, lattice bars. The small implant was manufactured from Ti6Al4V ELI (extra-low interstitial) using a Renishaw AM 250 selective laser melting (SLM) system. The nominal powder particle size was 15-45 µm. The lattice structure was manufactured from Ti6Al4V ELI using an Arcam Q10 electron beam melting (EBM) system. The nominal powder particle size was 45-100 µm. The methodology for the extraction of these surfaces from CT point cloud data is reported elsewhere [11, 12]. Data for the extracted surfaces, including captured re-entrant features (Sdr_{prime} and Sdr_{mesh}) are compared to projected (grid) data, Sdr_{ISO}. This grid data simulates data produced using a (perfect) line-of-sight instrument to measure the same

surface. This data will not include re-entrant information. Note: the Sdr_{prime} and Sdr_{mesh} calculation applied to grid data (height values projected onto a plane) produces the same result as Sdr_{ISO} for the same grid data. The values of these three parameters for two simulated structured surface examples are given and the robustness of the parameters, together with CT acquisition accuracy are discussed.

The CT measurement settings and the surface extraction procedure are discussed in section 2.1. The data processing and parameter generation are reported in section 2.2.

2.1 CT measurement and surface extraction

The SLM medical implant and the EBM lattice were both scanned on a Nikon XT H 225 CT. Reconstruction was performed using Nikon CT Pro 3D [13]. Surface determination was performed using VGStudio MAX 3.0 [14]. Local iterative surface determination was performed with a search distance of 4.0 voxels. Both surfaces were extracted using the VGStudio MAX 3.0 "Super Precise" setting and the file saved with a PLY format. The settings for the XT H 225 scan of the SLM medical implant are shown in Table 1.

Table 1 XT H 225 settings for the SLM medical implant scan

Parameter	Value	Parameter	Value
Filter	1 mm Cu	Voxel size	7.1 µm
Acceleration voltage	160 kV	Magnification	28.0
Filament current	62 µA	Detector size (pixels)	1008 x 1008
Exposure time	2829 ms	Number of projections	1583

An image of the extracted surface (PLY format) from the CT scan of the small medical implant surface is shown in Fig.3.
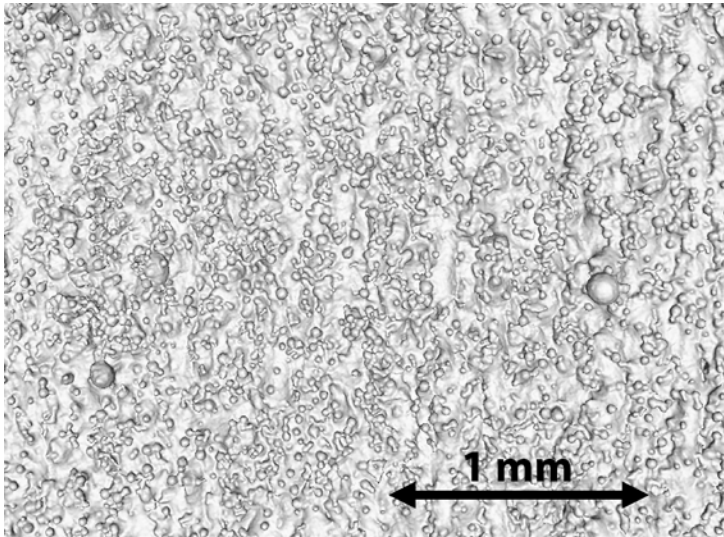

Fig.3 Extracted surface from SLM planar surface

The settings for the XT H 225 scan of the EBM lattice structure are shown in Table 2.

Table 2 XT H 225 settings for the EBM lattice structure scan

| Parameter	Value	Parameter	Value
Filter material	None	Voxel size	3.6 µm
Acceleration voltage	60 kV	Magnification	56.1
Filament current	100 µA	Detector size (pixels)	1008 x 1008
Exposure time	1000 ms	Number of projections	1583

The extracted lattice (PLY format) is shown in Fig.4. The region of intertest (ROI) used in the analysis is indicated in green. The dimensions for all figures are in mm.
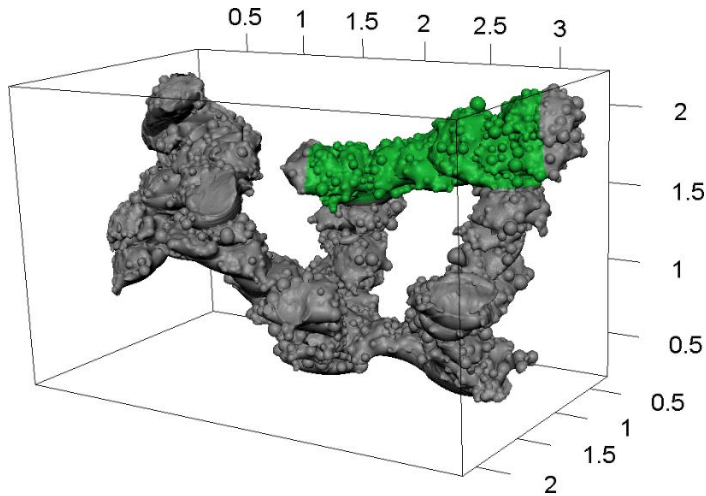
Fig.4 Extracted surface of the EBM scan of the lattice structure, showing the single bar region of interest used in the analysis

2.2 Data processing and generation of surface parameters

For the small Ti6Al4V ELI medical implant the extracted surface planar ROI is shown in Fig.5, showing the blue total least-squares reference plane.
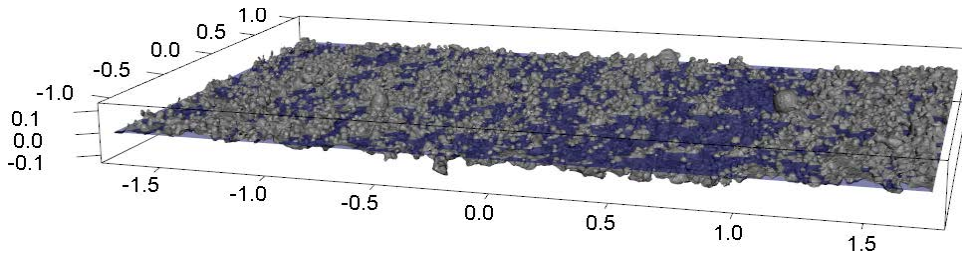
Fig.5 Extracted planar surface section of SLM small medical implant

The extracted ROI of the EBM lattice structure is shown in Fig.6. The reference cylinder is shown in blue. The cylinder was unwrapped prior to surface analysis.
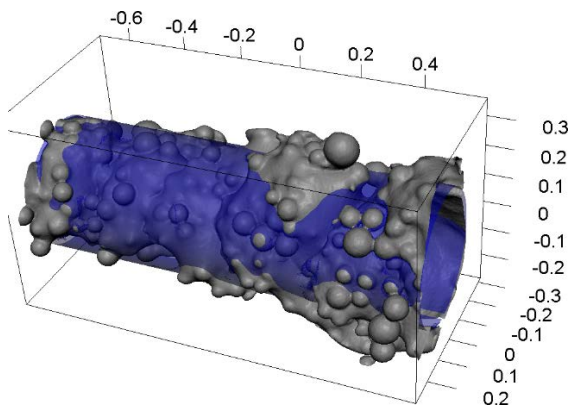
Fig.6 Extracted section of EBM lattice structure

2.2.1 Projected (grid) data

To generate data sets similar to those which would be produced by line-of-sight metrology techniques, such as optical focus variation and contact stylus profilometry, the extracted surface data was projected onto a grid (aligned with the datum planes). The grid spacing for the surface extracted from the SLM medical implant was 5 µm. The grid spacing for the surface extracted from the EBM lattice structure was 2 µm. This projection generates height-map data, with a single z value corresponding to an (x,y) location. This projection onto a grid produces as interpolated surface *curtain* where actual surface features are re-entrant, see Fig.7.
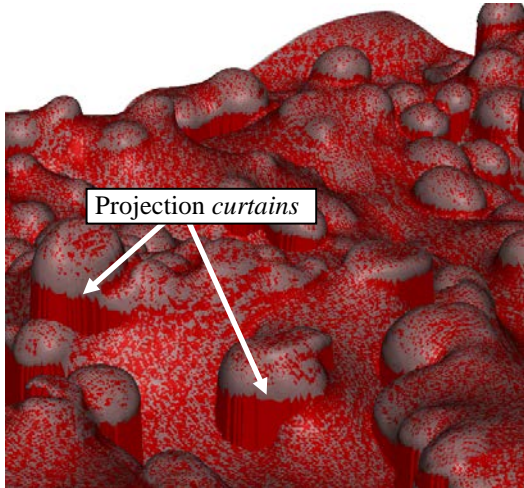
Fig.7 Detail of unwrapped EBM lattice, showing *curtains* caused by projection onto a grid

2.2.2 Comparison of projected (grid) and mesh data sets

Sdr_{ISO} surface data values can now be generated from this projected data, which has no information about re-entrant features, and this data can be compared to the true 3D mesh data to illustrate the potentially functionally significant errors produced when re-entrant features are not included in the surface parameter generation. Values of Sdr_{prime} and Sdr_{mesh} were generated for the AM surface CT 3D data sets and for the simulated structured surfaces. In all cases the primary (unfiltered) surface data sets were used in the comparison.

3 Results

3.1 Simulated surface examples

Two simulated structures are presented to illustrate the errors produced using projected (grid) data.

3.1.1 Simulated surface, example A

Fig.8**Error! Reference source not found.**(a) shows a CAD representation of a simulated structured surface, designed with intentional re-entrant features. The surface consists of repeated *mushroom* features. Each *mushroom* has a 4 mm diameter *cap*, with a 1 mm height, on a 1 mm diameter *stem*, with a 4 mm height. The envelope area is considered to be the top area of the cap, A_{cap}, 4π mm^2. This envelope area is used in the calculation of Sdr_{ISO} and Sdr_{prime}.

Sdr_{ISO} is the percentage of additional surface (using grid-projected data) contributed by the texture as compared to the area of a plane the size of the envelope area, 4π mm^2. The total projected surface area is

24π mm^2 (75.4 mm^2), which is the area of top face of the cap (4π mm^2) plus the area of the projection curtain, which is the circumference of the cap (4π mm) multiplied by the mushroom height, 5 mm. The calculated value of Sdr_{ISO} is therefore $(24 - 4)\,\pi\,/\,4\,\pi\,\times\,100\% = 500\%$.

Sdr_{prime} is the percentage of additional surface (including re-entrant surfaces) contributed by the texture as compared to the area of a plane the size of the envelope area. The actual surface area, including the surface area directly below the mushroom, is 61.3 mm^2. The value of Sdr_{prime} is therefore $(61.26 - 4\,\pi)\,/\,4\,\pi\,\times\,100\% = 387\%$.

Sdr_{mesh} is the percentage of additional surface (including re-entrant surfaces) contributed by the texture as compared to the area of a plane the size of the form area. The actual surface area, including the surface area directly below the mushroom, is 61.3 mm^2. The form area in this example is the area of the top of the *cap* + the area of the underside of the *cap* + the area of the *ground* directly beneath the *cap*, see Fig.2. This is equivalent to (3 x area of the *cap*) - (2x area of the *stem*) = $12\,\pi - \pi/2 = 11.5\,\pi$. Sdr_{mesh} is therefore $(61.26 - 11.5\,\pi)\,/\,11.5\,\pi\,\times\,100\% = 70\%$. The values of Sdr_{ISO}, Sdr_{prime} and Sdr_{mesh} are shown in Table 3. These results illustrate that the calculated surface area (and Sdr_{prime}), when re-entrant features are included may be less than the calculated surface when they are not included. As Sdr_{ISO} and Sdr_{prime} are percentage differences in relation to the envelope area, the error in Sdr_{ISO} (ie Sdr_{ISO} - Sdr_{prime}) is $500 - 387 = 113\%$ of the envelope area, over-estimating the actual surface area of the component.

Table 3 Single round *mushroom* extracted parameters

Method	Value
Sdr_{ISO}	500%
Sdr_{prime}	387%
Sdr_{mesh}	70%

Fig.8(b) shows the cumulative surface area, measured down from the top of the cap (100%) to the plane on which the *mushroom* sits (0%). Because there are no re-entrant features until 1 mm (80%) height, the line-of-sight and true 3D cumulative surface area values are identical. The transition to the *mushroom stem* occurs at 80% height, at which point the True 3D trace increases by the value of the surface area of the underside of the *cap*. The rate of increase of the True 3D surface area then reduces as the area of the *stem*, for a given height change, is less than the area of the outside of the *cap*. At the base of the *mushroom*, (0%), the True 3D area increases by the area of the *ground* surface directly below the mushroom cap. The line-of-sight interpolated surface *curtain* (see 1.0) is projected down from the top of the *mushroom cap*, and there is therefore no transition at 80% height, the increase of surface area for a given height change is constant from the top of the *mushroom* to the *ground* plane.
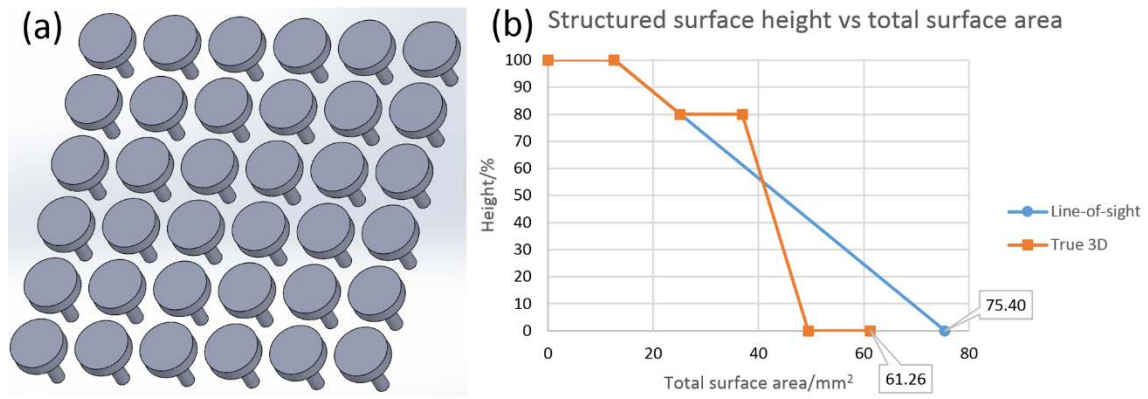
Fig.8 (a) structured surface, (b) graph of percentage height down from top vs total surface area

The material ratio curves for line-of-sight (Sdr_{ISO}) and true 3D (Sdr_{prime} and Sdr_{mesh}) are shown in Fig.9. The material ratio curve is the percentage area of material, at a given percentage of the surface height, compared to the envelope area. The envelope area, in this example, is the area of the *mushroom cap* top surface.
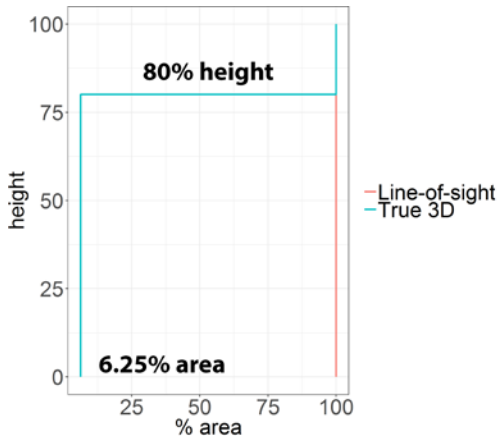

Fig.9 Material ratio curve, single structured round *mushroom*

The curve shows the material ratio for the line-of-sight data is constant, at 100%, from 100% height to 0% height. The True 3D curve indicates 100% material ratio from 100% height to 80% height, at which height the material ratio reduces to 6.25%, the percentage area of the *stem* in relation to the area of the *cap*. The material ratio curve does capture the (correct) True 3D data, and shows the line-of-sight and True 3D data are significantly different for this designed re-entrant feature. The material ratio curve, may provide useful functional information for analysing True 3D data sets, such those generated from CT measurements.

3.1.2 Simulated surface, example B

The second simulated *bench* sample was designed to illustrate the effect of structure configuration on the error in Sdr_{ISO}, compared with parameter Sdr_{prime}, see Fig.10. Sdr_{mesh} is shown for completeness. The cross section can be considered a (2 x 2) mm block on top of a (1 x 2) mm block, with *bench* length L. With these dimensions the value of Sdr_{ISO} is equivalent to $(8/L + 4) \times 100\%$, the value of Sdr_{prime} is equivalent to $(6/L + 5) \times 100\%$ and the value of Sdr_{mesh} is equivalent to $(3/L + 2) \times 100\%$.
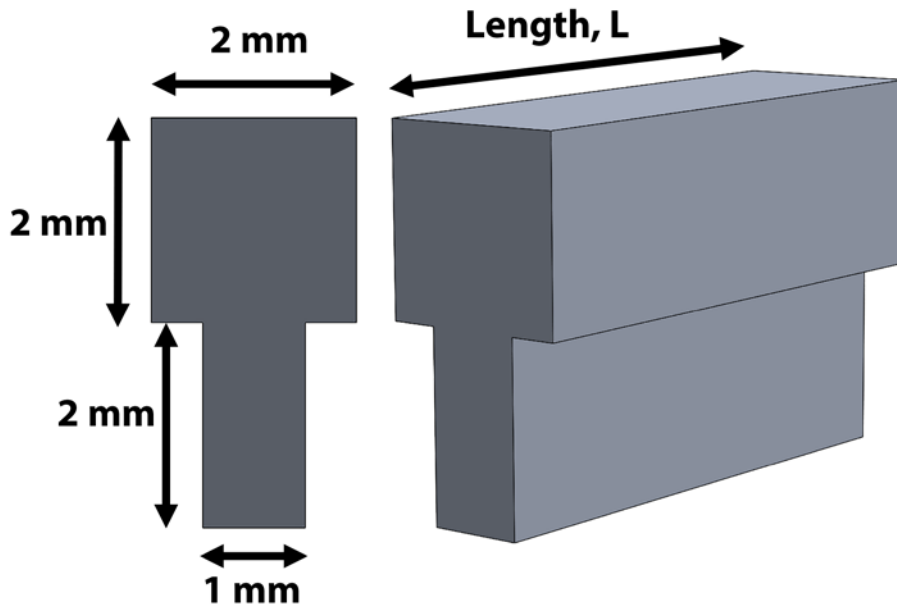
Fig.10 Views of the simulated *bench* artefact

Fig.11 shows the values of Sdr_{ISO}, Sdr_{prime} and Sdr_{mesh} for bench lengths ranging from 1 mm to 6 mm. It can be seen that the error of the Sdr_{ISO} changes from being positive (greater than Sdr_{prime}) to negative as the length increases. At a length of 2 mm the value corresponds to the Sdr_{prime} value. The curved shapes of the graphs is due to the effects of the end of the *bench*. The end-effect becomes less significant as the value of L increases. As L increases the value of Sdr_{prime} tends towards 500% and the value of Sdr_{ISO} tends towards 400%. This is an area error in Sdr_{ISO} equivalent to the areas of envelope area. The value of Sdr_{mesh} tends towards 200%.
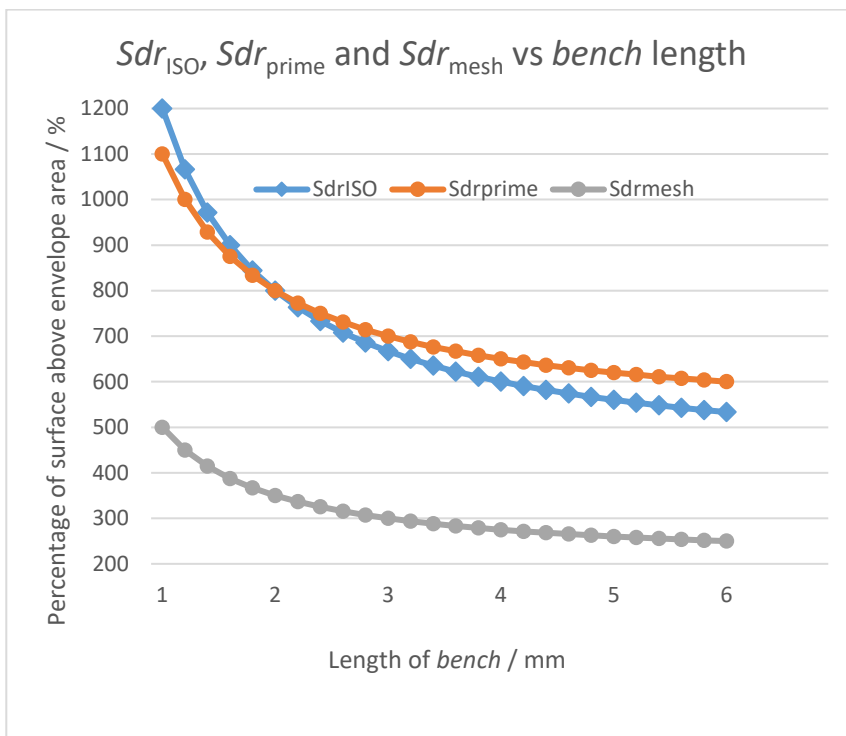
Fig.11 Graph of Sdr_{ISO}, Sdr_{prime} and Sdr_{prime} against *bench* length, L, showing equal values of Sdr_{ISO} and Sdr_{prime} at L = 2 mm

The material ratio curves for line-of-sight (Sdr_{ISO}) and true 3D (Sdr_{prime} and Sdr_{mesh}) are shown in Fig.12. The curves for the line-of-sight and True 3D data sets are again significantly different, however it should be noted that the material ratio curve for Sdr_{prime} (or Sdr_{ISO}) does not change as the value of *bench* length, L, increases from 1 mm to 6 mm. The material ratio curve is constant, however the value of Sdr_{prime} reduces from 1100% to 600% as L increases from 1 mm to 6 mm length. Therefore a combination of characterisation techniques, sensitive to the required component function and component surface changes, may be required to ensure acceptable component performance. If wear and friction are critical, for example, then the material area ratio is a good performance indicator.
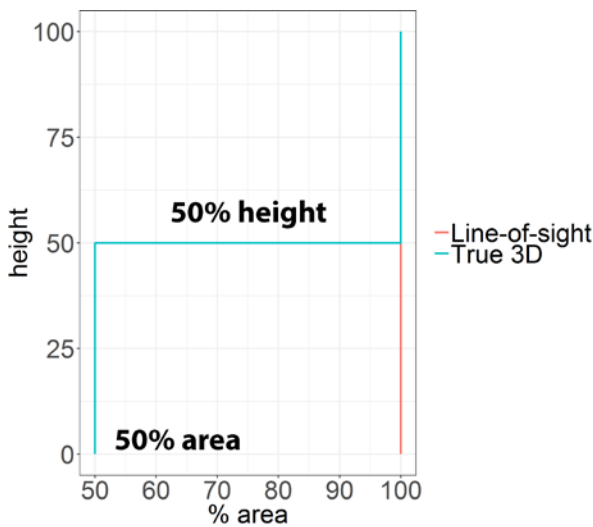
Fig.12 Material ratio curve for the simulated *bench*. Note: the material ration curve does not change as the bench length, L, changes

3.2 SLM medical implant surface

Table 4 shows the values of the three *Sdr* parameters for the SLM planar surface. The value of Sdr_{prime} is 79%, indicating the total actual surface area of the measured sample (including re-entrant features) is 79% more than the measured sample area. The value of Sdr_{ISO} is 68%, indicating that the line-of-sight analysis is underestimating the true surface area of the sample. This difference, 11% of the measurement area, may be significant for functional performance analysis, in this example, as it relates to bio-integration. Measurement of the surface of this SLM medical implant to include these re-entrant features, would be difficult or impossible with line-of-sight instrumentation. The value of Sdr_{mesh} for this sample is 55%. Unlike Sdr_{prime}, the value of Sdr_{mesh} cannot be directly related to the measurement area, see para. 1.1, and so it is less suitable for analysis of functional performance. The material ratio curve for the planar surface is shown in Fig.13. The curves shown are for height vs %area, the height value (y-axis) measured down from the maximum peak height for both line-of-sight and True 3D. The percentage total height was not used for the y-axis as the re-entrant features on some surfaces (True 3D) have been found to extend below the minimum line-of-sight height value. Therefore, when displayed as percentage of total height (y-axis), the area values (x-axis) do not refer to the same physical height on the sample. It can be seen that the value of percentage area for True 3D at a given height is always equal or less than the percentage area for the line-of-sight curve. The percentage will be equal when there are no re-entrant features, but at heights with

11

re-entrant features the True 3D area will account for the reduced area due to the undercut, whereas the line-of-sight will interpolate, creating a projection *curtain*, see Fig.1. This will produce an effective area larger than the true value.

Table 4 SLM planar surface texture parameters

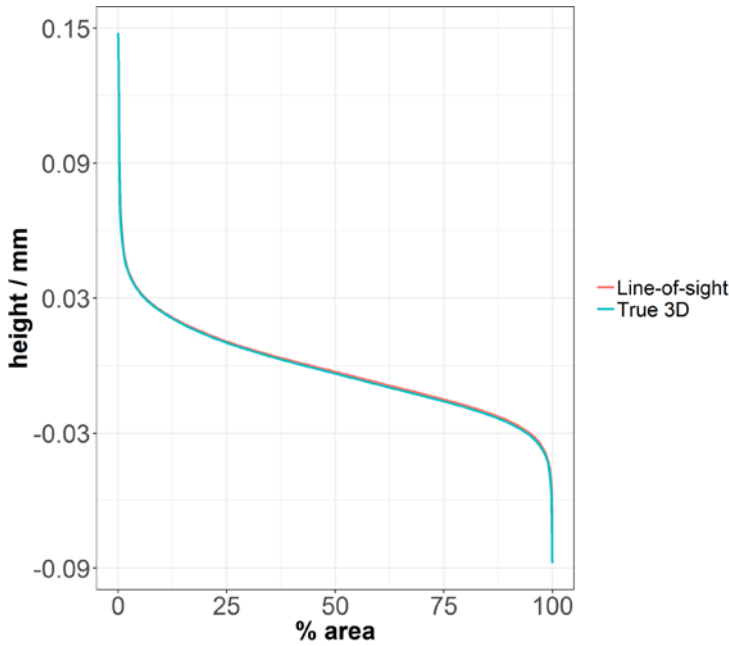| Method	Value
Sdr_{ISO}	68%
Sdr_{prime}	79%
Sdr_{mesh}	55%

Fig.13 Material ratio curve, SLM planar surface

3.3   EBM lattice structure

The values for the three *Sdr* parameters for the EBM lattice surface are shown in Table 5. Measurement of this simple lattice structure, and more complex multi-layer lattice structures, would not be possible with line-of-sight instrumentation. The value of Sdr_{prime} is 59%, indicating the total actual surface area of the measured sample (including re-entrant features) is 59% more than the measured sample area. The value of Sdr_{ISO} is 52%, indicating that the line-of-sight (equivalent) analysis is again underestimating the true surface area of the sample. The value of Sdr_{mesh} is 44%, again lower than the value of Sdr_{ISO}. Again, it is difficult to relate this figure to the physical surface, and therefore to the physical performance of the lattice in applications such as fluid heat transfer. The material ratio curve for the lattice structure is shown in Fig.14. The curves shown are height vs %area, the height value (y-axis) measured down from the maximum peak height for both line-of-sight and True 3D. As with the planar sample, para. 3.2, the value of area for True 3D is either equal or less than the line-of-sight area value. The difference between the line-of-sight and True 3D areas are greatest at heights between -0.03 and -0.06 mm, indicating this is the location of greatest re-entrant surface. This location information is not provided by the *Sdr* parameter values, illustrating the importance of selecting a suitable selection of parameters to fully characterise a surface.

12

Table 5 EBM lattice surface texture parameters

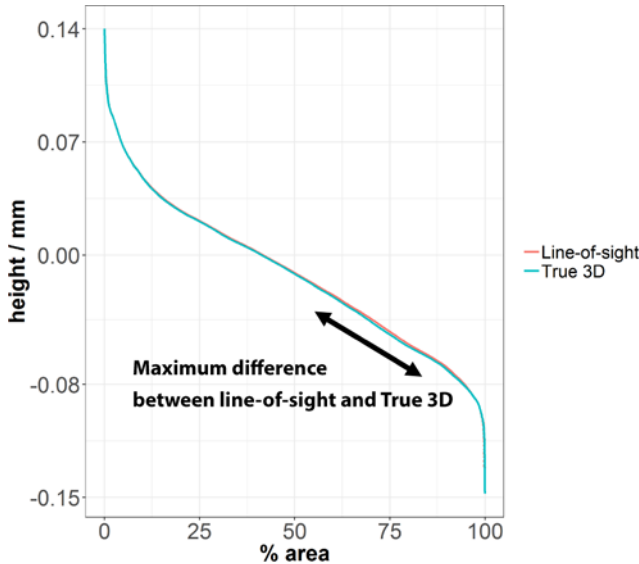| Method	Value
Sdr_{ISO}	52%
Sdr_{prime}	59%
Sdr_{mesh}	44%

Fig.14 Material ratio curve, EBM lattice

4   Discussion - measurement robustness and evaluation of measurement accuracy

Both evaluation methods based on the real 3D measured surface allow the characterisation of the re-entrant features. The Sdr_{mesh} is easier to compute on complex freeform surface, while the value of Sdr_{prime} is directly related to the designed surface, i.e. the presence of the re-entrant features increase the value of the parameter.

The ISO 4288 profile parameter, Ra, the *arithmetical mean deviation of the assessed profile* and the equivalent ISO 25178-2 areal surface texture parameter, Sa, the *arithemetical mean height of the scale-limited surface* are the most commonly used profile and areal surface roughness characterisation parameters resepectively. Significantly different surfaces (for example turned and ground) may have similar surface Ra and Sa values [15]. This is because one surface texture parameter cannot, in isolation, provide complete information about a surface. In practical use the accept / reject limits for a parameter are set with knowledge of the manufacturing process and are normally verified with practical performance verification (such as setting an Sa value range for a turned surface to be used with an elastomeric seal). This will also be the case for the numbers generated for Sdr_{prime} in a particular application: the accept / reject limits will be set based on particular verified functional performance. Depending upon the functional application additional information may be gained by utilising other surface texture parameters in addition to Sdr_{prime} to provide a more defined performance boundary. Future work will include investigation of functional applications of re-entrant surfaces and their correlation to Sdr_{prime} and Sdr_{mesh}.

Measurement accuracy for the extraction of as-built AM surface texture data from CT has been reported [11, 12]. The reported work included a processing step to convert the CT mesh data to a height map (grid)

13

format to allow direct comparison of the CT data to the reference line-of-sight focus variation instrument. The results indicated a difference between the surface extracted from CT and the same surface as measured on a reference focus variation instrument as small as 0.5 % for Sa. Measurement accuracy is dependent upon voxel size and surface texture roughness value. The resolution has to be sufficient to capture the required information at the required scales-of-interest [4]. It is expected that the accuracy and resolution limits will be similar for characterisation including the re-entrant features. Of course, it will not be possible to compare the accuracy of the characterisation of re-entrant surfaces using standard line-of-sight instruments as these will not capture the re-entrant data. Future work will include evaluation of measurement limits for a selection of functional re-entrant surfaces and verification of actual re-entrant surface configuration and Sdr_{prime} values compared to the surface-from-CT configuration, including sectioning AM components, similar to the methods utilised by Zanini et al. [16].

5   Conclusions

Powder bed fusion additive manufacturing processes are capable of producing complex freeform surfaces and re-entrant features that significantly enhance the designed function of the component in industrial applications including medical bio-attachment, electrical battery design, cooling and heating systems and paint and coating adhesion applications. The ability to measure and characterise these surfaces accurately will be vital to performance optimisation. However these surfaces present measurement and data analysis challenges that require the ability to image and extract meaningful data from complex true three-dimensional point clouds and meshes, such as those generated from CT measurements, rather than from a uniform height map grid typically generated by line-of-sight instrumentation. The ISO 25178-2 parameter Sdr (called Sdr_{ISO} in this work), used to analyse height map data, cannot be used to evaluate re-entrant surfaces accurately. The ISO parameter does, however, intentionally, relate directly to the surface envelope area, making it a useful functional analysis tool for non re-entrant surfaces, such as turned or milled surfaces. As has been discussed, Sdr_{mesh} can be used to analyse re-entrant surfaces, but, significantly, does not relate directly to the physical envelope of the component and so is not a good parameter for use in component functional perfromance analysis. As a consequence, a new parameter, Sdr_{prime} has been introduced. This parameter is the percentage of additional surface (including re-entrant surfaces) contributed by the texture as compared to a plane the size of the envelope area. This new parameter was developed to provide a direct relation to functional performance in these applications, where the inclusion of actual surface area from re-entrant features is critical. Existing parameters, including Sdr_{ISO} and Sdr_{prime} do not have this ability. CT scans of two AM surfaces have been made, capturing data for surfaces that would prove difficult or impossible to capture using line-of-sight measurements. Two example designed structured surfaces have been discussed. Values of Sdr_{prime} for the mesh (including re-entrant features) and generated projected grid data have been compared. It has been shown that there are significant errors in calculated area (up to 11% for Sdr_{prime}) when re-entrant features of as-built SLM and EBM additively manufactured components are not measured and included in analyses. Structured components, depending upon the design configuration, may have significantly greater errors due to line-of-sight projection, which will be included in any characterisation using the ISO 25178-2 parameter, represented here as Sdr_{ISO}. Utilisation of the novel techniques introduced here will allow the full potential of CT to be realised for the evaluation of re-entrant surfaces, providing the accurate data required for analysis and optimisation of functional performance, particularly suitable for additively manufactured as-built and structured surfaces.

14

References

[1]   E. Gyenge, S. Splinter, J. Jung, and A. Snaper, "High-specific surface area, three-dimensional reticulated electrodes for deep cycle lead-acid batteries," in *Seventeenth Annual Battery Conference on Applications and Advances. Proceedings of Conference (Cat. No.02TH8576),* 2002, pp. 19-24.

[2]   E. A. Silk, J. Kim, and K. Kiger, "Spray cooling of enhanced surfaces: impact of structured surface geometry and spray axis inclination," *International Journal of Heat and Mass Transfer,* vol. 49, no. 25, pp. 4910-4920, 2006.

[3]   C. Rungsiyakull, Q. Li, G. Sun, W. Li, and M. V. Swain, "Surface morphology optimization for osseointegration of coated implants," *Biomaterials,* vol. 31, no. 27, pp. 7196-7204, 2010.

[4]   A. Townsend, L. Pagani, L. Blunt, P. J. Scott, and X. Jiang, "Factors affecting the accuracy of areal surface texture data extraction from X-ray CT," *CIRP Annals - Manufacturing Technology,* 2017.

[5]   A. Thompson, L. Korner, N. Senin, S. Lawes, I. Maskery, and R. K. Leach, "Measurement of internal surfaces of additively manufactured parts by X-ray computed tomography," presented at the 7th Conference on Industrial Computed Tomography, Leuven, Belgium, 2017, 2017.

[6]   P. Müller, A. Cantatore, J. L. Andreasen, J. Hiller, and L. De Chiffre, "Computed tomography as a tool for tolerance verification of industrial parts," *Procedia CIRP,* vol. 10, pp. 125-132, 2013.

[7]   J.-P. Kruth, M. Bartscher, S. Carmignato, R. Schmitt, L. De Chiffre, and A. Weckenmann, "Computed tomography for dimensional metrology," *CIRP Annals-Manufacturing Technology,* vol. 60, no. 2, pp. 821-842, 2011.

[8]   W. W. Wits, S. Carmignato, F. Zanini, and T. H. Vaneker, "Porosity testing methods for the quality assessment of selective laser melted parts," *CIRP Annals-Manufacturing Technology,* vol. 65, no. 1, pp. 201-204, 2016.

[9]   *Geometrical product specifications (GPS) Surface texture: Areal - Part 2: Terms, definitions and surface texture parameters*, 2012.

[10]   L. Pagani, Q. Qi, X. Jiang, and P. J. Scott, "Towards a new definition of areal surface texture parameters on freeform surface," *Measurement,* vol. 109, no. Supplement C, pp. 281-291, 2017.

[11]   A. Townsend, L. Pagani, P. Scott, and L. Blunt, "Areal surface texture data extraction from X-ray computed tomography reconstructions of metal additively manufactured parts," *Precision Engineering,* vol. 48, no. Supplement C, pp. 254-264, 2017/04/01/ 2017.

[12]   A. Townsend *et al.*, "An interlaboratory comparison of X-ray computed tomography measurement for texture and dimensional characterisation of additively manufactured parts," *Additive Manufacturing,* vol. 23, pp. 422-432, 2018/10/01/ 2018.

[13]   Nikon metrology NV, "Nikon CT Pro 3D."

[14]   Volume Graphics GmbH, "VGStudio MAX."

[15]   L. Mummery, *Surface texture analysis: the handbook.* Hommelwerke Mulhausen, 1990.

[16]   F. Zanini, M. Sorgato, and S. Carmignato, "Experimental investigation on the accuracy of surface topography measurements of additively manufactured metal parts scanned by X-ray micro computed tomography," presented at the Joint special interest group meeting between euspen and ASPE, KU Leuven, Belgiuim, October 2017, 2017.